Zirconium Phosphate: The Pathway from Turbostratic Disorder to Crystallinity

Aida Contreras-Ramirez‡, Songsheng Tao†, Gregory S. Day‡, Vladimir I. Bakhmutov‡, Simon J. L. Billinge†⊥ and Hong-Cai Zhou* §‡.*

‡ Department of Chemistry, Texas A&M University, College Station, TX 77843, USA

† Department of Applied Physics and Applied Mathematics, Columbia University, New York, NY 10027.

§Department of Materials Science and Engineering, Texas A&M University, College Station, Texas 77843-3003, United States.

⊥ Condensed Matter Physics and Materials Science Department, Brookhaven National Laboratory, Upton, NY 11973

Supplementary Information

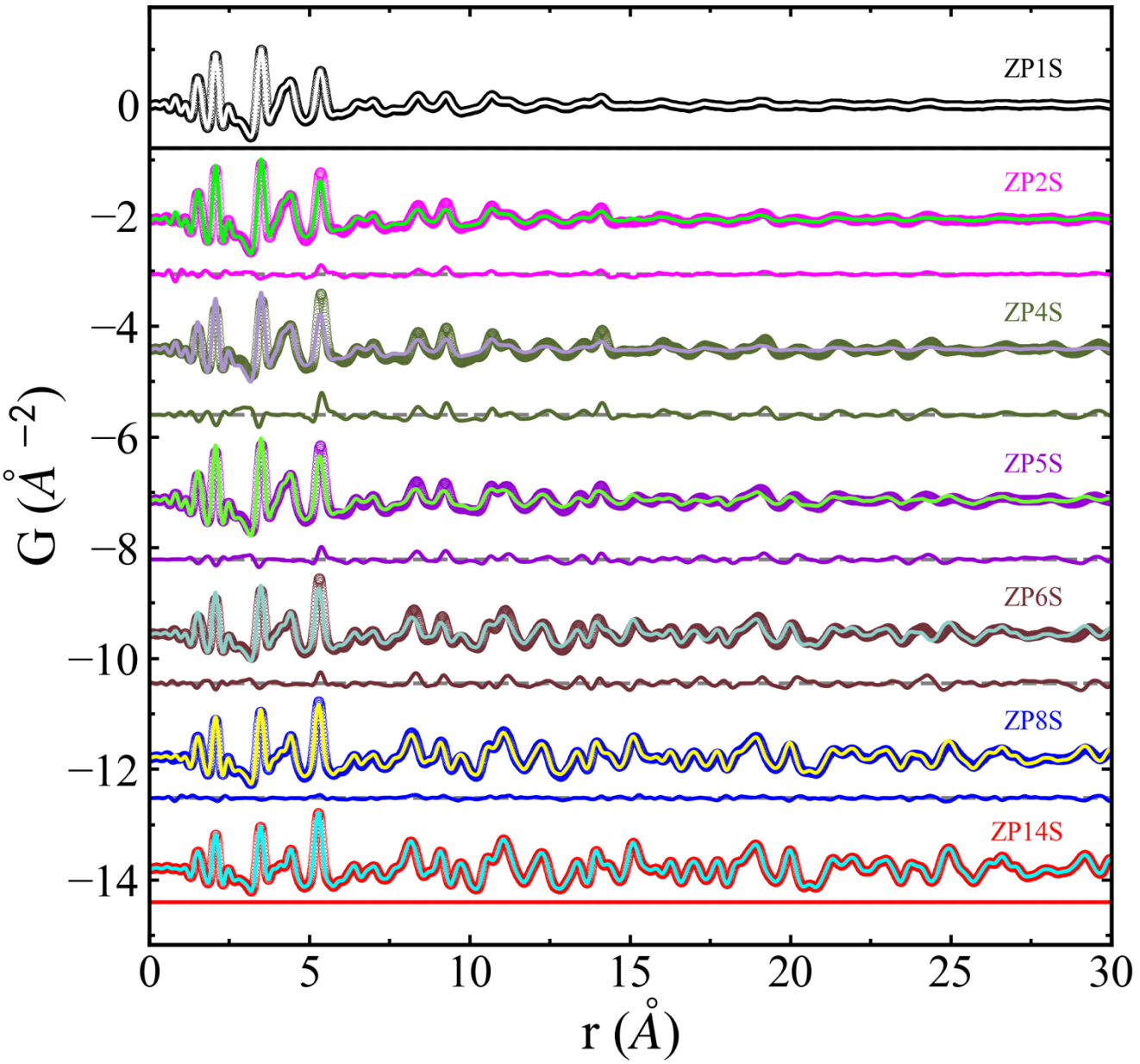

Figure S1. Experimental PDFs of S-series (empty dots) and fitted linear combination of PDFs of ZP1S and ZP14S (solid line) with the difference curves below.

Table S1. Refined parameters in S-series.

	ZP1S	ZP2S	ZP4S	ZP5S	ZP6S	ZP8S	ZP14S
$scale_{bulk}$	0.466	0.302	0.138	0.110	0.315	0.242	0.363
psize (Å)	8.324	8.968	17.432	61.511	88.754	230.307	281.749
a (Å)	10.089	9.758	9.841	9.189	9.121	9.069	9.069
b (Å)	5.221	5.291	5.439	5.278	5.295	5.289	5.283
c (Å)	13.918	14.268	15.299	15.383	15.419	15.394	15.390
β_{bulk}	108.026	107.712	108.431	101.124	101.641	101.700	101.653
U_{Zr}^{bulk} (Å^{-2})	0.002	0.005	0.004	0.007	0.006	0.007	0.005
U_{P}^{bulk} (Å^{-2})	0.000	0.000	0.002	0.006	0.006	0.006	0.005
U_{O}^{bulk} (Å^{-2})	0.016	0.031	0.054	0.041	0.031	0.027	0.023
$scale_{layer}$	0.183	0.230	0.259	0.285	0.266	0.138	0.119
x scale	1.005	1.009	1.017	1.009	1.006	1.001	1.011
y scale	0.996	1.015	1.011	1.017	1.006	1.006	0.989
z scale	1.000	0.980	0.967	0.977	0.993	0.992	1.004
U_{Zr}^{layer} (Å^{-2})	0.008	0.009	0.007	0.010	0.008	0.012	0.017
U_{P}^{layer} (Å^{-2})	0.009	0.013	0.009	0.006	0.004	0.023	0.023
U_{O}^{layer} (Å^{-2})	0.016	0.027	0.029	0.038	0.022	0.047	0.053
δ (Å)	1.834	1.912	1.826	1.927	1.913	3.230	3.260

Figure S2 shows the different FT-IR spectra for αZrP prepared by the stirring, reflux, and hydrothermal methods. The FT-IR spectrum for ZP8R and ZP14H200 show a broad stretching band typical of water at 3600-2500 cm^{-1} and a bending band (δ(H-O-H)) at 1620 cm^{-1}. A weak shoulder at 1245 cm^{-1} is attributed to (ν(P=O)). The large and broad band at 1020 cm^{-1} corresponds to the symmetric stretching of P-O bond in the PO_4 group and a shoulder at 950 cm^{-1} to (δ(P-OH)). The bands at 600 cm^{-1}, 460 cm^{-1} and 400 cm^{-1} are attributed to the Zr-O bond.[1-4]

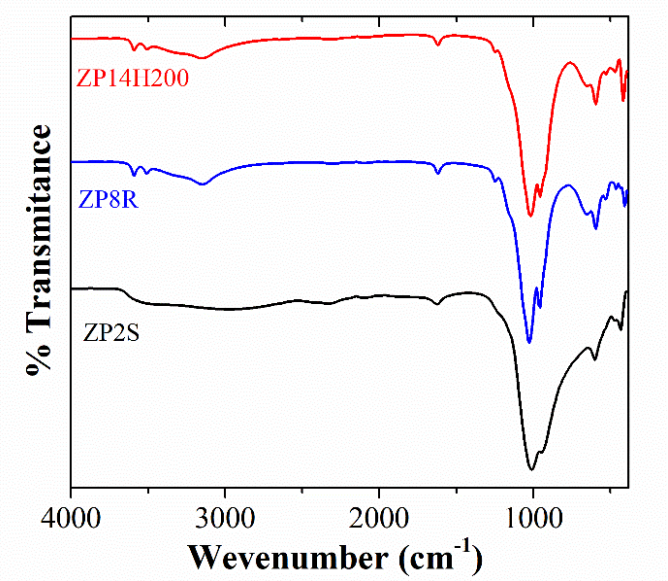

Figure S2. FT-IR spectra for ZrP prepared by stirring, hydrothermal, and reflux methods.

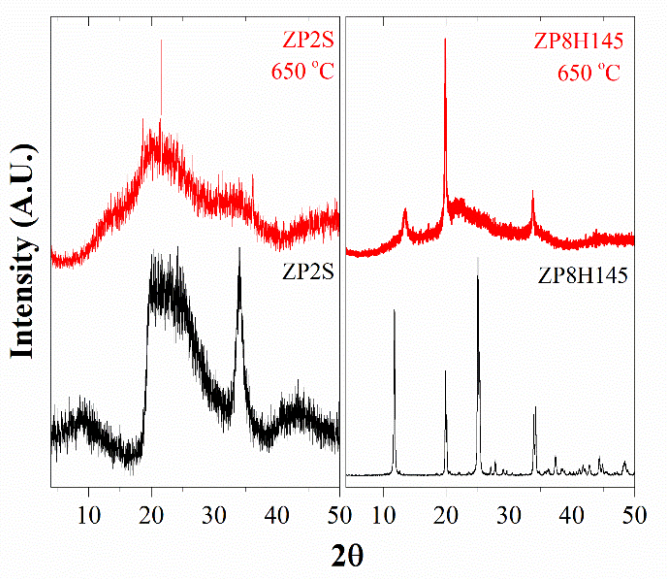

Figure S3. PXRD pattern of ZP2S an ZP8H145 after annealing at 650 oC for 2 hours.

The FT-IR spectra for the samples after temperature treatment are presented in Figure S4. From 4000 cm^{-1} to 1800 cm^{-1} no bands are observed. The assignment of the $P_2O_7^{4-}$ modes are given in terms of PO_3 and P-O-P vibration.[5] The symmetric and asymmetric stretching frequencies of PO_3 are observed in the 1157-1100 cm^{-1} region. For P-O-P, symmetric modes were observed around 760 cm^{-1}. The bands between 590 and 440 cm^{-1} are attributed to δ O-P-O, δPO_3 and δ P-O-P deformations.[5-6] These spectra demonstrate the formation of ZrP_2O_7 in the turbostratic and in the crystalline samples.

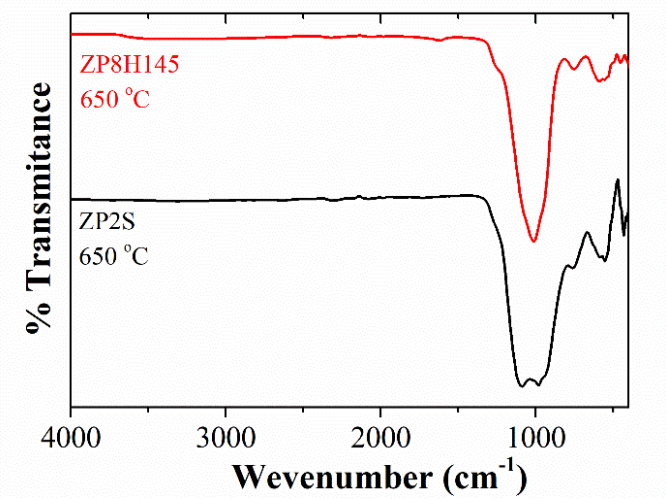

Figure S4. FT-IR spectra for ZP2S and ZP8H145 after annealing at 650 oC for 2 hours.

The $^{31}P\{^{1}H\}$ MAS NMR spectrum of ZP2S (Figure S5), recorded at a spin rate of 4 kHz, shows a major resonance at -23.4 ppm due to orthophosphate (HPO_4^{2-}). A short and well-defined peak at -15.3 ppm could be attributed to the resonance of phosphate within a more hydrated area. Meanwhile, a shoulder to the right of the main resonance, -29.1 ppm, could be attributed to a dehydrated phase of ZrP.[7-8] The wide peaks on the spectrum suggest that the material is not homogeneous, which is in good agreement with the PDF data.

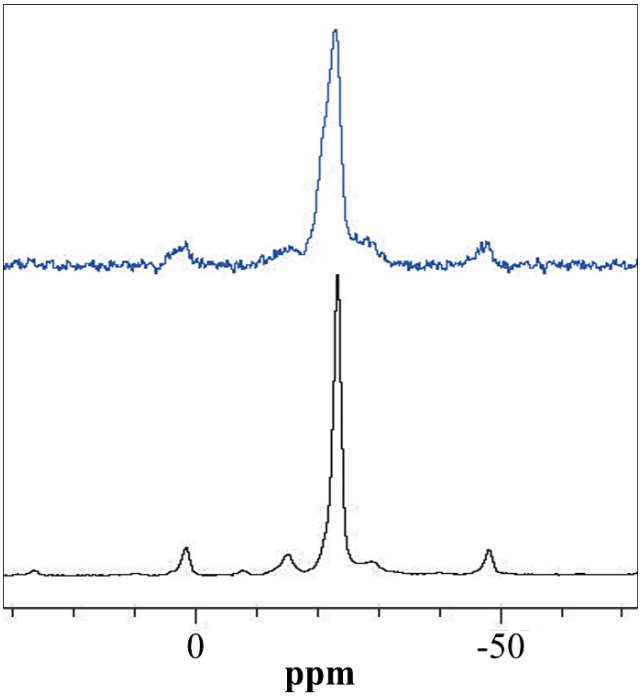

Figure S5. $^{31}P\{^{1}H\}$ MAS NMR spectra of ZP2S at a spinning rate of 4 kHz from top to bottom: the spectrum obtained with direct excitation of 31P nuclei; the spectrum obtained with proton-phosphorus cross polarization.

The ^{1}H MAS NMR spectrum of αZrP is shown in Figure S6. The ^{1}H MAS NMR spectrum of ZP2S and ZP8H200 at a spin rate of 5.1 kHz. As expected, this spectrum is not informative due to strong proton-proton dipolar interactions. Nevertheless, the ^{1}H MAS NMR spectrum for ZP8H200 (bottom) shows a major resonance at 6.1 ppm and a second resonance at 7.6 ppm, these resonances belong to protons of water situated between layers and also protons P−OH (b).[9] ZP2S spectrum (top) shows two resonances at 8.4 and 6.3 ppm, which can be assigned to protons of water and HPO_4^{2-} groups.

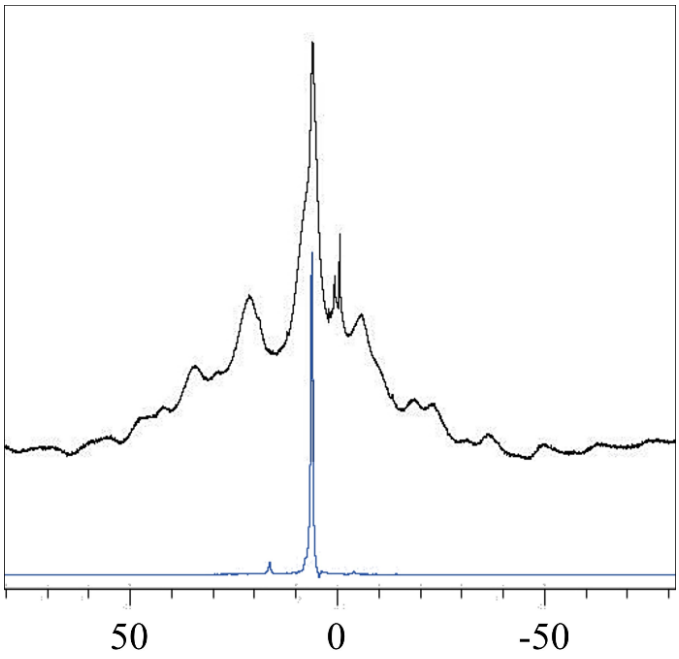

Figure S6. The 1H MAS NMR spectrum of ZP2S(top), ZP8H200(bottom) spinning at a rate of 5.1 kHz.

Table S2. Refined parameters in H-series.

	ZP2H 90	ZP2H 145	ZP2H 200	ZP8H 90	ZP8H 145	ZP8H 200	ZP14H 90	ZP14H 145	ZP14H 200
$scale_{bulk}$	0.566	0.51	0.451	0.397	0.373	0.401	0.439	0.339	0.431
psize (Å)	51.769	62.471	136.642	187.487	135.484	260.767	154.904	116.416	108.336
a (Å)	9.09	9.077	9.063	9.066	9.07	9.067	9.075	9.073	9.093
b (Å)	5.322	5.312	5.289	5.288	5.292	5.289	5.298	5.296	5.315
c (Å)	15.333	15.342	15.393	15.409	15.401	15.411	15.368	15.398	15.316
β_{bulk}	101.659	101.693	101.709	101.707	101.711	101.707	101.743	101.71	101.837
U_{Zr}^{bulk} ($Å^{-2}$)	0.005	0.005	0.005	0.005	0.005	0.005	0.005	0.005	0.005
U_{P}^{bulk} ($Å^{-2}$)	0.005	0.005	0.005	0.004	0.004	0.004	0.005	0.004	0.005
U_{O}^{bulk} ($Å^{-2}$)	0.009	0.009	0.012	0.012	0.011	0.013	0.011	0.011	0.011

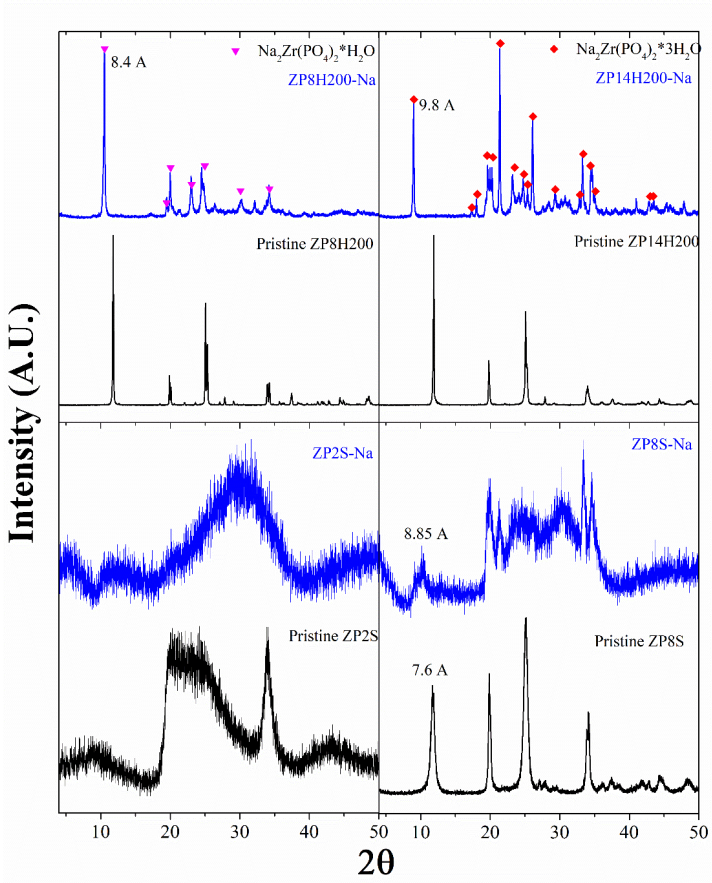

Figure S7. PXRD pattern of pristine ZrP alongside the material after Na^+ ion exchange.

Figure S8 illustrates the identical ^{31}P $\{^{1}H\}$ MAS NMR spectra obtained by direct ^{31}P excitation and proton-phosphorus cross polarization, of the sample ZP8H200. Showing that the phosphorus groups are surrounded by the same number of protons. Two signals are observed, one at -19.5 (very small) and another -21.2 ppm (in a ratio of 1 to 19) in full accordance with the data reported earlier for αZrP.[10-11] Both signals belong to HPO_4^{2-} orthophosphate groups located in more (-19.5 ppm) and less (-21.2 ppm) hydrated areas of αZrP. The most important feature of the spectra is the fact that in the sample of higher crystallinity, the major signal is narrower with a linewidth of 60-70 Hz.

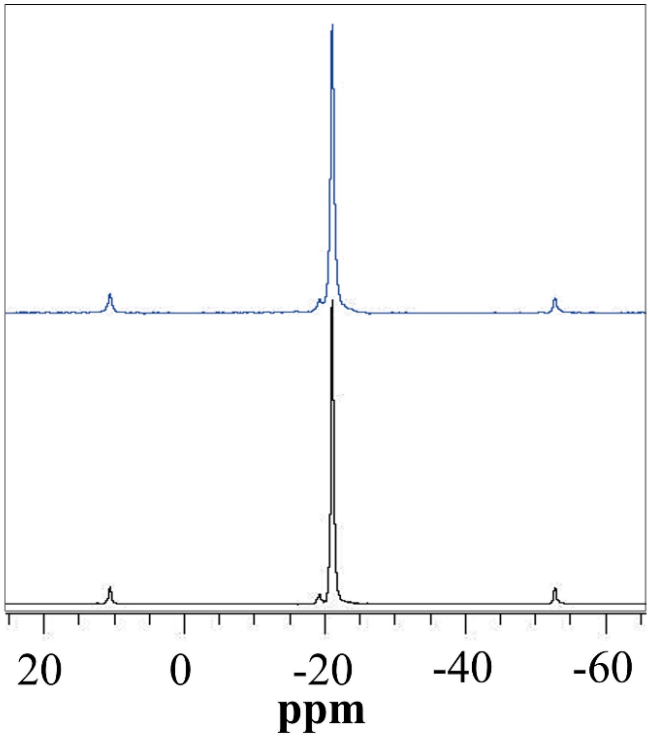

Figure S8. 31P{1H} MAS NMR spectra of ZP8H200 at a spinning rate of 5.1 kHz from top to bottom: the spectrum obtained with direct excitation of 31P nuclei; the spectrum obtained with proton-phosphorus cross polarization.

To support this conclusion, we performed the $^{31}P\{^{1}H\}$ CP MAS NMR experiments both with and without the spin-lock section shown in Figure S9. The ^{1}H spin-lock X CP MAS NMR spectra manifest X resonances developed due to cross polarization via protons characterized by the longest ^{1}H $T_{1\rho}$ times. Generally, the X CP signals at the ^{1}H spin-lock are associated with a crystalline phase, while the spectral difference shows an amorphous phase.[12] As seen in Figure S6, the spectral difference is quite small, supporting the high crystallinity of the sample.

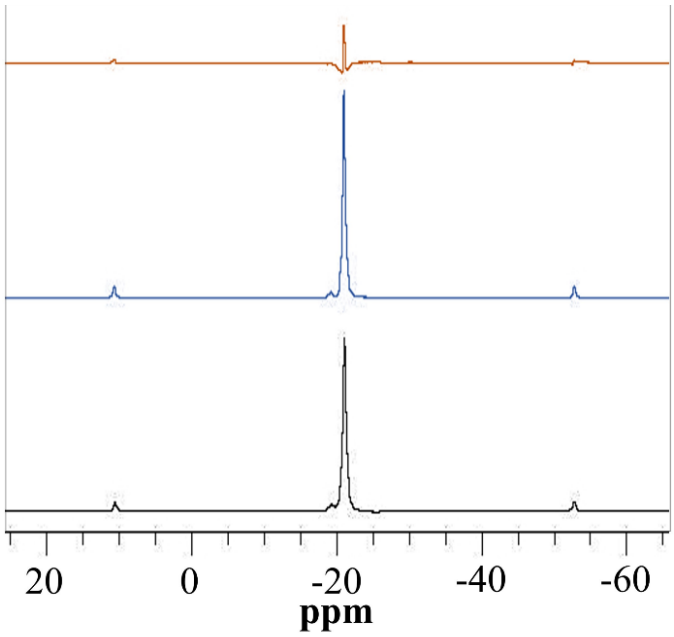

Figure S9. 31P{1H} CP MAS NMR spectrum (middle) and 31P{1H} 1H spin-lock CP MAS NMR spectrum at a spin-lock pulse length of 16 ms (bottom) recorded for sample ZP8H200, spinning at a rate of 5 kHz, the top spectra show the difference between the two.

Figure S10 shows the high resolution XPS spectra for P 2p and Zr 3d, for ZP14H200 and ZP2S samples. The P $2p_{3/2}$ and $2p_{1/2}$ peaks overlap, giving one peak centered at 134.4-134.2 eV, respectively (Figure S7 a). The Zr $3d_{5/2}$ and $3d_{3/2}$ peaks are centered at 183.8-183.6 and 186.2-186.1 eV (Figure S7 b), these values are in strong agree with values previously reported.[13-14] The high-resolution scans for the Zr 3d and P 2p regions in the well crystallized sample (ZP14H200) show an increase in binding energy of ~0.2 eV which indicates a difference in polarization. The binding energies are referenced to the C 1s line, which was fixed at 284.8 eV. The spectrum has been fitted using Gaussian, after a Shirley-type back ground subtraction.

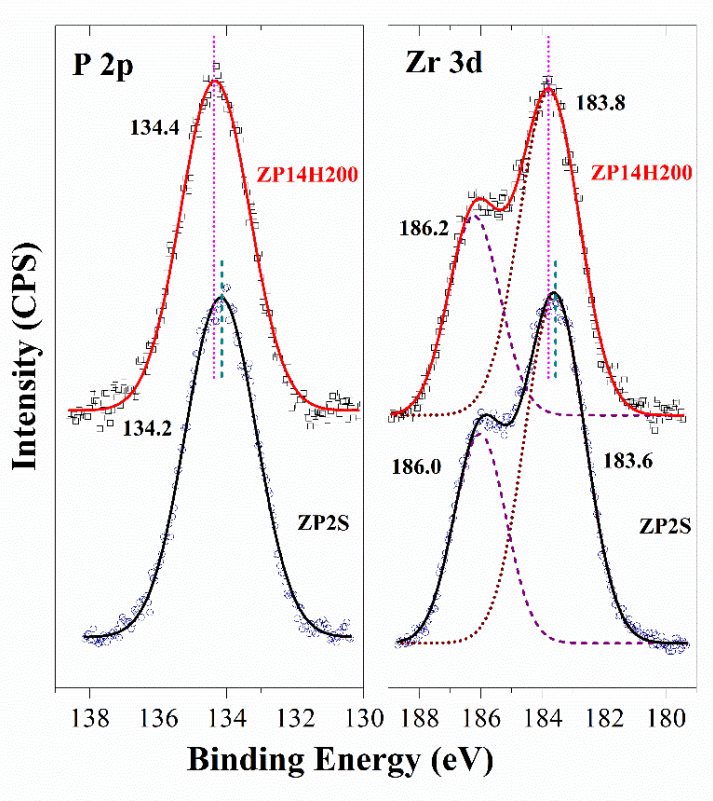

Figure S10. X-ray photoelectron spectra of ZP2S and ZP14H200: a) P 2p binding energy region; b) Zr 3d3/2 and Zr 3d5/2 binding energy region.

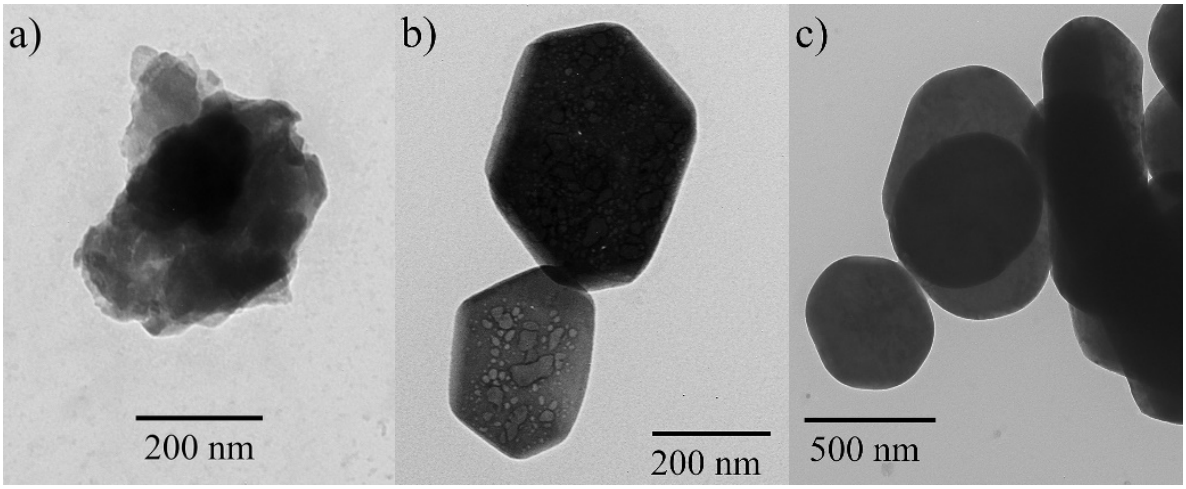

Figure S11. TEM images of H-samples series: a) ZP2H145, b) ZP8H145, c) ZP14H145.

Table S3. Refined parameters in R-series.

	ZP2R	ZP8R	ZP14R
$scale_{bulk}$	0.2	0.505	0.459
psize (Å)	25.471	152.354	177.744
a (Å)	9.143	9.081	9.073
b (Å)	5.452	5.452	5.452
c (Å)	15.002	15.345	15.416
b_{bulk}	101.179	101.731	101.644
U_{Zr}^{bulk} (Å^{-2})	0.003	0.006	0.005
U_{P}^{bulk} (Å^{-2})	0.003	0.005	0.005
U_{O}^{bulk} (Å^{-2})	0.035	0.023	0.021
$scale_{layer}$	0.337	0.165	0.157
x scale	1.004	1.01	1.007
y scale	0.994	0.995	0.997
z scale	1.205	1.002	1.003
U_{Zr}^{layer} (Å^{-2})	0.011	0.013	0.02
U_{P}^{layer} (Å^{-2})	0.007	0.024	0.052
U_{O}^{layer} (Å^{-2})	0.028	0.059	0.101
d (Å)	2.038	3.305	3.358

References

1. Frey, B. L.; Hanken, D. G.; Corn, R. M., Vibrational Spectroscopic Studies of the Attachment Chemistry for Zirconium Phosphonate Multilayers at Gold and Germanium Surfaces. *Langmuir* **1993,** *9*, 1815-1820.
2. Bortun, A. I.; Khainakov, S. A.; Bortun, L. N.; Jaimez, E.; Garcia, J. R.; Clearfield, A., Synthesis and Characterization of a Novel Layered Tin(IV) Phosphate With Ion Exchange Properties. *Mater Res Bull* **1999,** *34*, 921-932.
3. Stuart, B. H., *Infrared Spectroscopy: Fundamntals and Applications*. 2004.
4. Jaimez, E.; Bortun, A.; Hix, G. B.; Garcia, J. R.; Rodriguez, J.; Slade, R. C. T., Synthesis of Phosphate-Phenylphosphonates of Titanium(IV) and Their n-Butylamine Intercalates. *J Chem Soc Dalton* **1996**, 2285-2292.
5. Seyyidoglu, S.; Ozenbas, M.; Yazici, N.; Yilmaz, A., Investigation of solid solution of ZrP2O7-Sr2P2O7. *J Mater Sci* **2007,** *42* (15), 6453-6463.
6. Guler, H.; Kurtulus, F., A microwave-assisted route for the solid-state synthesis of lead pyrophosphate, Pb2P2O7. *J Mater Sci* **2005,** *40* (24), 6565-6569.

7. Pica, M.; Donnadio, A.; Capitani, D.; Vivani, R.; Troni, E.; Casciola, M., Advances in the Chemistry of Nanosized Zirconium Phosphates: A New Mild and Quick Route to the Synthesis of Nanocrystals. *Inorg Chem* **2011,** *50* (22), 11623-11630.
8. Mosby, B. M.; Diaz, A.; Bakhmutov, V.; Clearfield, A., Surface Functionalization of Zirconium Phosphate Nanoplatelets for the Design of Polymer Fillers. *Acs Applied Materials & Interfaces* **2014,** *6*, 585-592.
9. Bakhmutov, V. I.; Clearfield, A., P-31, H-1 NMR Relaxation and Molecular Mobility in Layered alpha-Zirconium Phosphate: Variable-Temperature NMR Experiments. *Journal of Physical Chemistry C* **2017,** *121* (1), 550-555.
10. Segawa, K.; Nakajima, Y.; Nakata, S.; Asaoka, S.; Takahashi, H., P-31-Masnmr Spectroscopic Studies with Zirconium-Phosphate Catalysts. *J Catal* **1986,** *101* (1), 81-89.
11. Clayden, N. J., Solid-State Nuclear-Magnetic-Resonance Spectroscopic Study of Gamma-Zirconium Phosphate. *J Chem Soc Dalton* **1987,** (8), 1877-1881.
12. Hietala, S.; Maunu, S. L.; Sundholm, F.; Jamsa, S.; Viitaniemi, P., Structure of thermally modified wood studied by liquid state NMR measurements. *Holzforschung* **2002,** *56* (5), 522-528.
13. Alberti, G.; Costantino, U.; Marletta, G.; Puglisi, O.; Pignataro, S., ESCA Investigations of Amorphous and Crystalline Zirconium Acid Phosphates. *J Inorg Nucl Chem* **1981,** *43*, 3329-3334.
14. Sanchez, J.; Ramos-Garces, M. V.; Narkeviciute, I.; Colon, J. L.; Jaramillo, T. F., Transition Metal-Modified Zirconium Phosphate Electrocatalysts for the Oxygen Evolution Reaction. *Catalysts* **2017,** *7*.